Identification of Mono- and Bisubstrate Inhibitors of Protein Farnesyltransferase and Inducers of Apoptosis from a Pepticinnamin E Library

Michael Thutewohl,[a] Lars Kissau,[a] Boriana Popkirova,[b] Ionna-Maria Karaguni,[b]
Thorsten Nowak,[c] Michael Bate,[c] Jürgen Kuhlmann,[b]
Oliver Müller[b] and Herbert Waldmann[a,*]

[a]*Max-Planck-Institut für molekulare Physiologie, Abt. Chemische Biologie, Otto-Hahn-Str. 11,
D-44227 Dortmund und Fachbereich 3, Organische Chemie, Universität Dortmund, Germany*
[b]*Max-Planck-Institut für molekulare Physiologie, Abt. Strukturelle Biologie, Otto-Hahn-Str. 11, D-44227 Dortmund, Germany*
[c]*AstraZeneca, Mereside, Alderley Park, Macclesfield, Cheshire SK10 4TG, UK*

Abstract—A library of 51 analogues of the naturally occurring protein farnesyltransferase inhibitor pepticinnamin E was investigated biologically. Several compounds with pronounced inhibitory activity were discovered with the lowest IC_{50} value reaching 1 μM. The library contains inhibitors which are competitive to either farnesylpyrophosphate or the peptide substrate and a bisubstrate inhibitor. This activity is supported and rationalized by molecular modelling experiments and different binding modes of the inhibitors deduced from them. Several compounds induced apoptosis in a Ras-transformed tumour cell line, and in one case this correlated with farnesyltransferase-inhibiting activity.
© 2003 Elsevier Science Ltd. All rights reserved.

Introduction

Mutations in the genes encoding for Ras proteins are found in ca. 30% of all human tumours.[1,2] In order to exert their biological functions the Ras proteins must be *S*-farnesylated at the C-terminus.[3] Thus, inhibitors of the enzyme protein farnesyltransferase (PFT) are of particular interest. PFT catalyses the transfer of the lipid group to a cysteine residue embedded in the C-terminal CAAX-box of a non-matured Ras protein (Scheme 1). However, although this application of signal transduction therapy[4] has led to clinical examination of several farnesyltransferase inhibitors some of the most important and fundamental issues determining their biological activity remain unclear. Thus, the crucial substrate(s) of PFT the farnesylation of which is

C = Cys   A = aliphat. amino acid   Far =

X = Met, Ser, Gln
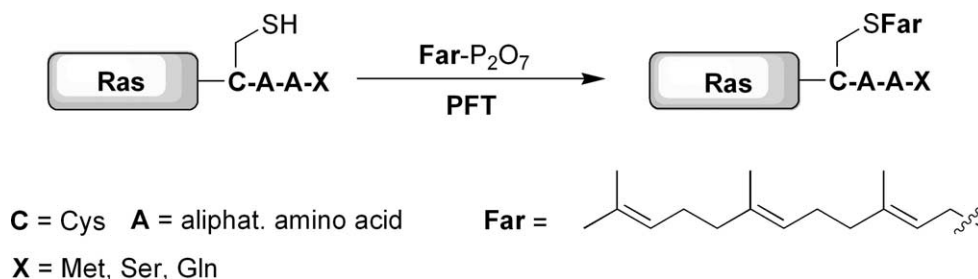
Scheme 1. The farnesylation of ras by protein farnesyltransferase (PFT).

*Corresponding author. Tel.: +49-231-133-2400; fax: +49-231-133-2499; e-mail: herbert.waldmann@mpi-dortmund.de
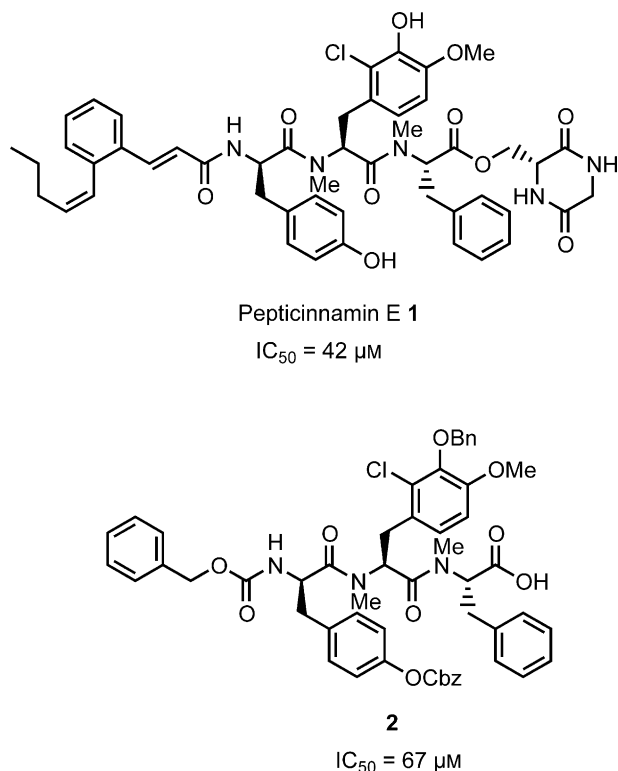
Figure 1. The bisubstrate inhibitor pepticinnamin E 1 and analogue 2.

suppressed is not known.[2] Also, the apoptosis-inducing activity of PFT inhibitors has not yet been traced to a molecular target.

To investigate these biological questions, bisubstrate inhibitors of PFT are considered particularly relevant.[5–7] Based on the structure of pepticinnamin E 1[8] (Fig. 1), a naturally occurring bisubstrate inhibitor of PFT[9] and analogue 2 which is similar in potency to the natural product we have developed a solid-phase synthesis of a library of potential PFT inhibitors.[10] The synthesis is detailed in the accompanying paper.[10b] Here, we describe the biological evaluation of this compound collection and the delineation of a structure activity relationship.

Results and Discussion

The library of pepticinnamin E analogues was subjected to two complementary assays for their potential inhibitory activity towards PFT. In the first assay[11] tritium-labelled farnesylpyrophosphate and the K-Ras protein were used as substrates and human placental PFT as enzyme. The assay was adapted to the 96-well plate format, the degree of inhibition was determined after precipitation of the labelled proteins. For compounds which displayed > 50% inhibition at 30 μM IC$_{50}$ values were determined (see Tables 1–3). In addition, a fluorescence-based assay using rat PFT and a dansyl-labelled Ras peptide[12] embodying a CAAX-sequence was adapted to the 96-well plate format.[13] For compounds which showed > 50% inhibition at 50 μM, IC$_{50}$ values were determined (see Tables 1–3).

The synthesized compounds can be grouped into three categories: (i) compounds with a backbone similar to the natural product (Table 1, entries 3–22), (ii) compounds with aromatic side chains similar to pepticinnamin E but not N-methylated (Table 2, entries 1–5 and Table 3, entries 3 and 4), (iii) compounds embodying histidine as N-terminal amino acid (Table 2, entries 6–27 and Table 3, entries 1 and 2). Analysis of group (i) reveals that compounds composed of four or five building blocks and carrying a hydrophobic alkyl- or alkenyl substituted phenyl ring at the N-terminus that might mimic the farnesyl group mostly are inactive (Table 1, entries 3–5 and 7–9). Only compounds 6, 10 and 11 display considerable activity. Notably, pepticinnamin E itself and analogue 2 did not show any appreciable inhibitory activity under the assay conditions employed in this study (Table 1, entries 1 and 2). Compounds 12–22 have a shortened N-acyl group. Among these 16 and 17 display IC$_{50}$ values in the low micromolar range. Direct comparison of these two compounds with non-N-methylated analogues (Table 2, entries 1–5) underscores the importance of the N-methylation.

Notably, the active compounds identified from group (ii) all have a carboxylic acid at the C-terminus, esterification or amide formation are not beneficial.
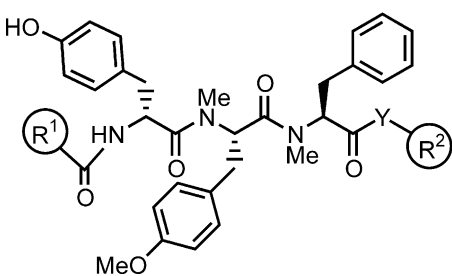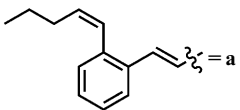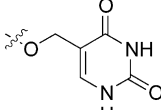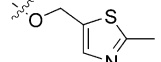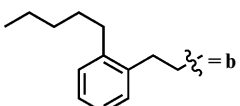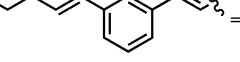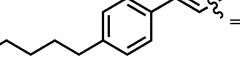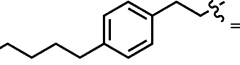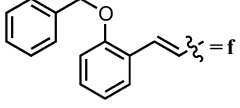
The largest group of analogues (iii) carries a histidine as N-terminal amino acid to promote binding to the zinc ion in the active site of PFT[14] (see below; Table 2, entries 6–27, Table 3, entries 1 and 2). Indeed in this group several active compounds were identified with IC$_{50}$ values down to the single-digit micromolar level. Direct comparison of, for example, 23 with 30 proves that this is due to the presence of the imidazole ring.

In addition to the introduction of the histidine moiety the group summarized in Table 2 and in entries 1 and 2 of Table 3 displays variations in the configuration of the N-terminal amino acid, the degree of N-methylation and the structure of the N-substituent. Trends apparent from inspection of the corresponding data are that in the presence of longer N-acyl chains the configuration of the N-terminal amino acid and the degree of N-methylation appear to be less important (Table 2, entries 11–21, compare entries 12 and 15 as well as entries 13 and 14). For the Z-substituted analogues at least one N-methylation appears to be required for high activity with prefer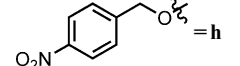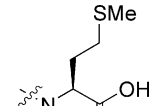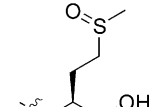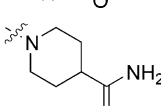ence for a D-configured histidine (entries 6–8), and if the Z-urethane is exchanged for a hydrocinnamic acid activity drops.

Furthermore acylation of unmethylated His-Phe-Tyr with benzyloxy-substituted cinnamic acid derivatives yielded appreciable inhibitory activity (Table 2, entries 22–27) but in these cases a clear correlation of activity and structure was not apparent.
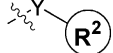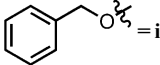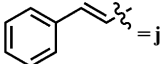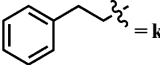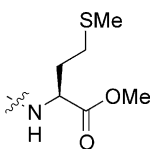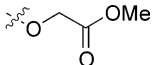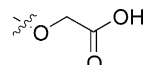
From these data it can be concluded that for efficient inhibition either a histidine at the N-terminus is required or in non-histidine peptides two N-methyl groups should be present. In both cases the structure of the N-terminal substituent is an important modulating element.

Table 1. Screening results for compounds **3–22**

Entry	Compd	R^1	Y–R^2	FTase[a] (IC$_{50}$) (μM)	FTase[b] (IC$_{50}$) (μM)	MDCK-f3 apoptosis inhib. concn (%)
1	**1**			112		
2	**2**			[c]		
3	**3**	= a		—[d]	> 30	—[f]
4	**4**	a		—[d]	> 30	—[f]
5	**5**	a	–OH	> 50	57%[e]	—[f]
6	**6**	= b	–OH	> 50	6.4	50[g]; 100[h]
7	**7**	= c	–OH	—[d]	> 30	100[h]
8	**8**	= d	–OH	—[d]	> 30	100[h]
9	**9**	= e	–OH	—[d]	> 30	100[h]
10	**10**	= f	–OH	9.3	57%[e]	—[f]
11	**11**	Fm = g	–OH	16.0		
12	**12**	= h		42.4		
13	**13**	h		> 50		
14	**14**	h		28.2		
15	**15**	h	–OH	> 50	> 30	

(continued on next page)

Table 1 (*continued*)

Entry	Compd	R[1]	Y–R[2]	FTase[a] (IC$_{50}$) (μM)	FTase[b] (IC$_{50}$) (μM)	MDCK-f3 apoptosis inhib. concn (%)
16	**16**	(benzyloxy) = **i**	–OH	5.3	6.7	—[f]
17	**17**	(cinnamyl) = **j**	–OH	16.2	12.8	
18	**18**	(phenethyl) = **k**	(Met-OMe amide, SMe)	> 50	> 30	
19	**19**	**k**	(O–CH$_2$–CO–OMe)	—[d]	> 30	—[f]
20	**20**	**k**	(O–CH$_2$–CO–OH)	36.3	> 30	—[f]
21	**21**	**k**	–OAll	—[d]	> 30	
22	**22**	**k**	–OH	> 50	> 30	

Fm, Fluorenylmethyl-.
[a] Fluorescence-test against rat-PFT.[12]
[b] Radioactive test against human PFT.[13]
[c] No observed inhibition at 200 μM substance concentration.
[d] No observed inhibition at 50 μM substance concentration.
[e] 57% inhibition at 50 μM substance concentration.
[f] No observed apoptosis at 100 μM substance concentration.
[g] Apoptosis at 50 μM substance concentration.
[h] Apoptosis at 100 μM substance concentration.

In order to rationalize these results, molecular modelling experiments were carried out. To this end, the X-ray structure of rat farnesyltransferase in complex with farnesyl pyrophosphate (FPP) and the substrate peptide CVFM[15,16] was investigated. In Figure 2a, it is shown that in this complex the farnesyl group (blue) is bound in a hydrophobic pocket (green) while the phosphate group (red) interacts with a hydrophilic surface and is close to a zinc ion (magenta) which also binds to the SH group of the cysteine in the CAAX peptide. The N-terminal amino acid binds to a hydrophobic pocket while the C-terminal amino acid interacts with basic amino acids of the protein (the peptide binding pocket is shown in yellow). Figure 2b shows the hydrophobicity map of the active site with the binding sites for the farnesyl group the phosphate and the carboxylate. The map was created with HYDROMAP.[16]
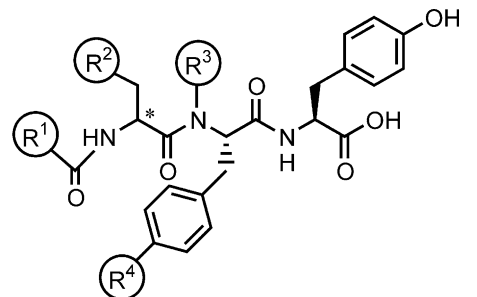
Docking of the identified inhibitors into the active site was initially investigated with automatic docking programs which did not lead to meaningful results. Instead manual docking was applied supported by hydrophobicity maps for the active site (Fig. 2b) and the inhibitors which were constructed with WitnotP.[22]

Figure 3a displays the binding mode proposed for pepticinnamin E with this approach. Both the FPP binding site and the peptide binding site are occupied by the unpolar cinnamic acid residue and the polar amino acid side chains, respectively.

Figure 3b and c shows the proposed binding modes of compounds **16** and **10** carrying a benzyloxycarbonyl group and an *ortho*-benzyloxycinnamic acid amide. By analogy to pepticinnamin E the methoxyphenyl group blocks the pyrophosphate binding site. The zinc ion comes close (3.64 Å for **16** and 3.56 Å for **10**) to the N-terminal aromatic group, probably by interaction with the π-system. The hydrophobic FPP binding site is occupied by the Z-urethane and the benzyloxycinnamic acid substituent. Both inhibitors block the lower part of the active site but the peptide binding pocket is only partially occupied and should be accessible for a substrate peptide. This was confirmed by subsequent kinetic studies (see below). These binding modes may be employed to rationalize the observed inhibitory activities. Thus, **7**, **8** and **9** differ only in the N-terminal substituent. Docking of these compounds into the active site by analogy to the binding mode proposed for **10** leads to strong repulsive interactions with the *meta*- and *para*-substituents of the aromatic rings.

Figure 3d shows the proposed binding mode for histidine-containing peptide **45**. The histidine is coordinated to the zinc ion (2.4 Å distance, which is close to literature data[17]), and the *meta*-benzyloxycinnamoyl group

Table 2. Screening results for compounds **23–49**

Entry	Compd	R1	R2	*	R3	R4	PFT[a] IC$_{50}$ (μM)	PFT[b] IC$_{50}$ (μM)	MDCK-f3 apopt. inhib. concn (%)
1	23	(benzyl ether) = **i**	HOPh–	D	Me	H	> 50	> 30	
2	24	**i**	HOPh–	D	H	H	> 50	> 30	—[d]
3	25	**i**	HOPh–	D	H	OH	—[c]	> 30	
4	26	**i**	HOPh–	L	H	OH	—[c]	> 30	
5	27	**i**	Ph–	L	H	H	24.0	> 30	
6	28	**i**	Imid	L	H	H	> 50	> 30	
7	29	**i**	Imid	L	Me	H	13.3	30.5	—[d]
8	30	**i**	Imid	D	Me	H	8.0	6.4	—[d]
9	31	(4-nitrobenzyl ether, O$_2$N) = **l**	Imid	D	H	H	57.9	1.1	—[d]
10	32	(4-pentyl styryl) = **d**	Imid	D	H	H	—[c]	> 30	—[d]
11	33	**d**	Imid	D	H	H	8.1		
12	34	(4-pentyl phenethyl) = **e**	Imid	D	H	H	9.3		
13	35	**e**	Imid	L	H	H	7.1	1.1	—[d]
14	36	**e**	Imid	L	Me	H	11.6	16.9	
15	37	**e**	Imid	D	Me	H	10.5		—[d]
16	38	(4-pentenyl styryl) = **l**	Imid	D	H	H	31.0		
17	39	(3-pentenyl styryl) = **c**	Imid	D	H	H	31.2		
18	40	(2-pentenyl styryl) = **a**	Imid	D	H	H	24.4		
19	41	(2-pentyl phenethyl) = **b**	Imid	D	H	H	31.6		
20	42	(biphenyl phenethyl) = **m**	Imid	D	H	H	52.4		
21	43	(biphenyl styryl) = **n**	Imid	D	Me	H	7.7	22.1	
22	44	*ortho* (BnO-styryl) = **o**	Imid	D	H	H	15.3	1.0	—[d]

Table 2 (*continued*)

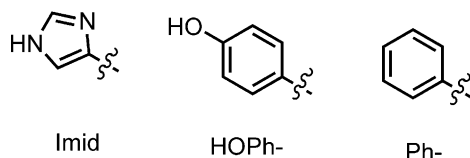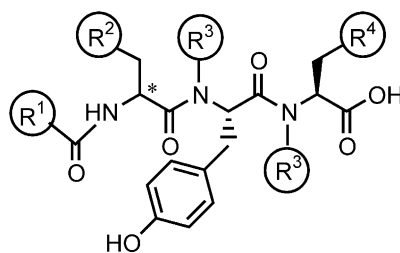| Entry	Compd	R¹	R²	*	R³	R⁴	PFT[a] IC$_{50}$ (μM)	PFT[b] IC$_{50}$ (μM)	MDCK-f3 apopt. inhib. concn (%)
23	**45**	*ortho* **o**	Imid	L	H	H	6.4	19.2	—[d]
24	**46**	*meta* **o**	Imid	L	H	H	12.5		
25	**47**	*meta* **o**	Imid	D	H	H	> 50	7.6	
26	**48**	*para* **o**	Imid	L	H	H	8.2		
27	**49**	*para* **o**	Imid	D	H	H	23.1	4.1	

[a]Fluorescence-test against rat-PFT.[12]
[b]Radioactive test against human PFT.[13]
[c]No observed inhibition at 50 μM substance concentration.
[d]No observed apoptosis at 100 μM substance concentration.

Imid   HOPh-   Ph-

.

Table 3. Screening results for compounds **50–53**

Entry	Compd	R¹	R²	*	R³	R⁴	FTase[a] (IC$_{50}$) (μM)	FTase[b] (IC$_{50}$) (μM)	MDCK-f3 apoptosis inhib. concn (%)
1	**50**	= **i**	Imid	L	Me	Ph	> 50	> 30	—[c]
2	**51**	= **k**	Imid	L	Me	Ph	> 50	> 30	—[c]
3	**52**	= **e**	HOPh–	D	H	Ph	24.0	> 30	—[c]
4	**53**	**e**	HOPh–	D	H	Naph	> 50	> 30	100

[a]Fluorescence-test against rat-PFT.[12]
[b]Radioactive test against human PFT.[13]
[c]No observed apoptosis at 100 μM substance concentration.

blocks the FPP binding site. In the binding mode shown, part of the FPP binding site and part of the peptide binding pocket are occupied so that compound **45** might be a bisubstrate inhibitor. This mode of action was confirmed by kinetic evaluation (see below).

Figure 3e shows the proposed binding mode for **37** which was obtained using the same procedure. Here, the peptide adopts a confirmation in which the peptide binding site is blocked but the FPP-binding site remains unoccupied so that this compound should not be competitive to FPP.

In order to determine whether the hints gleaned from the modelling experiments concerning the possible modes of inhibition for differently substituted pepticinnamin E analogues can be substantiated, compounds **10**, **16**, **30**, **37** and **45** were subjected to kinetic studies employing the fluorescence-based assay described above.
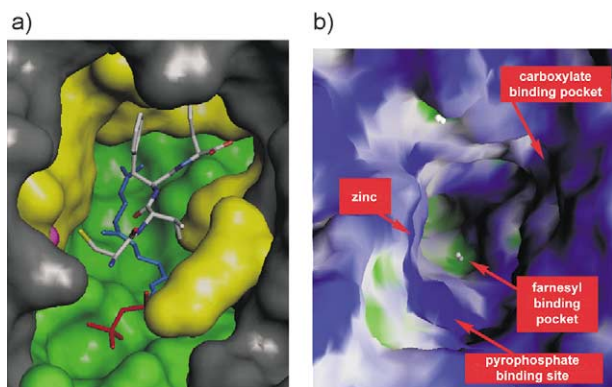
Figure 2. Points of interaction between ligand and receptor in the active site of farnesyltransferase: (a) crystal structure of rat farnesyltransferase with CVFM peptide and farnesylpyrophosphate; (b) hydrophobicity map of the substrate binding site of PFT.

Figure 4 shows the Lineweaver–Burk plots determined for these five inhibitors for varying concentration of FPP and dansyl-peptide. Figure 4a and b clearly show that compound **45** is a bisubstrate inhibitor as was expected in the light of the modelling results. Histidine-containing inhibitors **30** and **37** are competitive to the peptide substrate but not to FPP. This also is in accordance with the modelling result described for **37** above.

In addition, compounds **16** and **10** proved to be competitive to FPP, and also in this case the experimental data confirm the conclusions drawn from the modelling experiments (see Fig. 4g and i).

In Figure 4d, f, h and j the recorded values decrease with increasing dansyl-peptide concentration but in the absence of inhibitor. This unusual but reproducible observation indicates substrate inhibition that has been recorded for DansGCVLC before.[18]
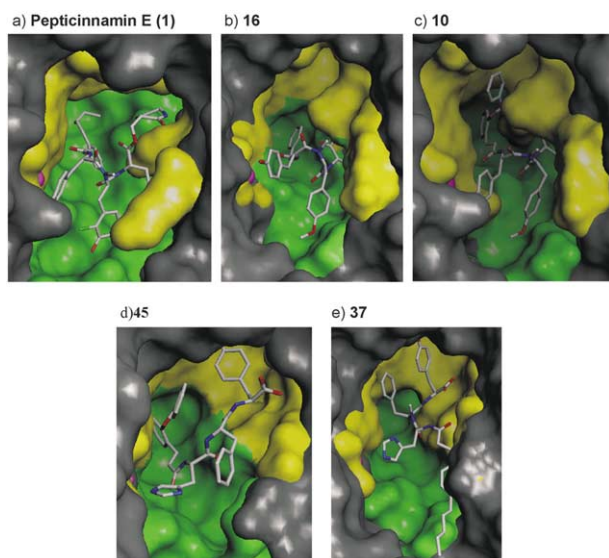

Figure 3. Inhibitors **1** (a), **16** (b), **10** (c), **45** (d), **37** (e) in the active site of PFT determined by molecular modelling experiments.

Finally, the most promising candidates identified were examined with an assay developed by us[19] for their ability to induce apoptosis in Ras-transformed cells but not in the corresponding wilde-type cells. In this assay, MDCK-f3 tumour cells from dog kidney were used, which are transfected with oncogenic H-Ras.[20] The transformed MDCK-f3 cells differ from the corresponding non-transformed cells in various morphological parameters. While the wild-type cells are round-shaped, adhere and form colonies (Fig. 5a), transformed cells are spindle-shaped, do not adhere and grow irregularly (Fig. 5b). A cell-division-inhibiting, morphology-changing or apoptosis-inducing effect of a substance on MDCK-f3 cells indicates an influence on the Ras signal-transduction cascade.

After incubation for 6 h and subsequent staining of the cell components the results were analysed by fluorescence microscopy. Although several compounds had displayed appreciable PFT-inhibitory activity in the in vitro assays (see above) most of them were inactive at 100 µM concentration, and the tumour cells remained spindle-shaped (not shown). However, compounds **6–9** and **53** induced apoptosis of the MDCK-f3 cells.

These pepticinnamin E analogues are tripeptides embodying aromatic amino acids—but not histidine—and carry *N*-acyl groups with long lipophilic chains.

At 100 µM, **7–9** induce an early stage of apoptosis indicated by rounding of the cells (Fig. 5c–e). At this concentration, compounds **6** and **53** induce the final stage of apoptosis which is accompanied by rounding of the cells and fragmentation of the nucleus (Fig. 5f and g). At 50 µM concentration, compound **53** had no effect anymore whereas compound **6** induced an early stage of apoptosis (Fig. 5 h). At 20 µM concentration, both compounds induced no visible change. In comparison, experiments under identical conditions and with different concentrations[21] the wild-type MDCK cells showed no apoptotic effect (see Fig. 5i and j; the cells colonies are intact). Thus these compounds are not generally cytotoxic and the observed apoptosis is due to an influence on the Ras signalling pathway.

We note, however, that in the PFT assays only compound **6** had displayed marked inhibitory activity. Thus, the other compounds appear to have (a) different biological target(s). The elucidation of this problem is subject to ongoing research activities.

Conclusion

A library of 51 pepticinnamin analogues was investigated as potential inhibitors of protein farnesyltransferase. Twenty compounds displayed pronounced inhibitory activity with the best IC_{50} value reaching 1 µM. Kinetic experiments revealed that the library contains inhibitors which are competitive to the peptide substrate, farnesylpyrophosphate or to both substrates. These findings are in full accord with the proposed binding modes of the inhibitors to the enzyme, delineated with molecular modelling experiments.
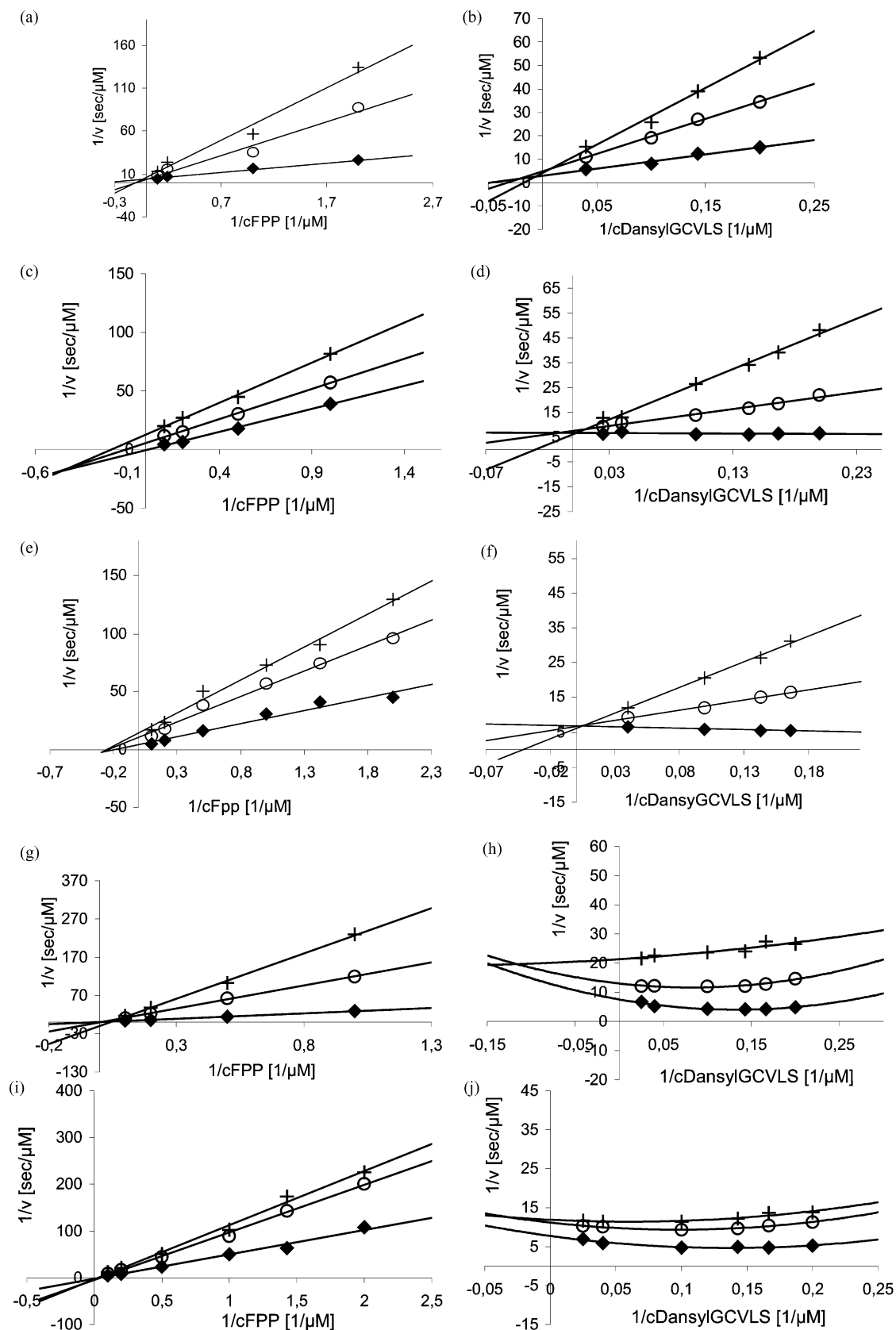
Figure 4. Inhibition of Rat-PFT by inhibitors **45** (a, b), **30** (c, d), **37** (e, f), **16** (g, h) and **10** (i, j); (a), (c), (e), (g), (i): Lineweaver–Burk plot with FPP as varied substrate with constant concentration of DansGCVLS of 10 μM. Concentration of the appropriate inhibitor: 0 (◆), 10 (○) and 20 (+) μM; (b), (d), (f), (h), (j): Lineweaver–Burk plot with DansGCVLS as varied substrate with constant concentration of FPP of 10 μM. Concentration of the appropriate inhibitor with 0 (◆), 10 (○) and 20 (+) μM.
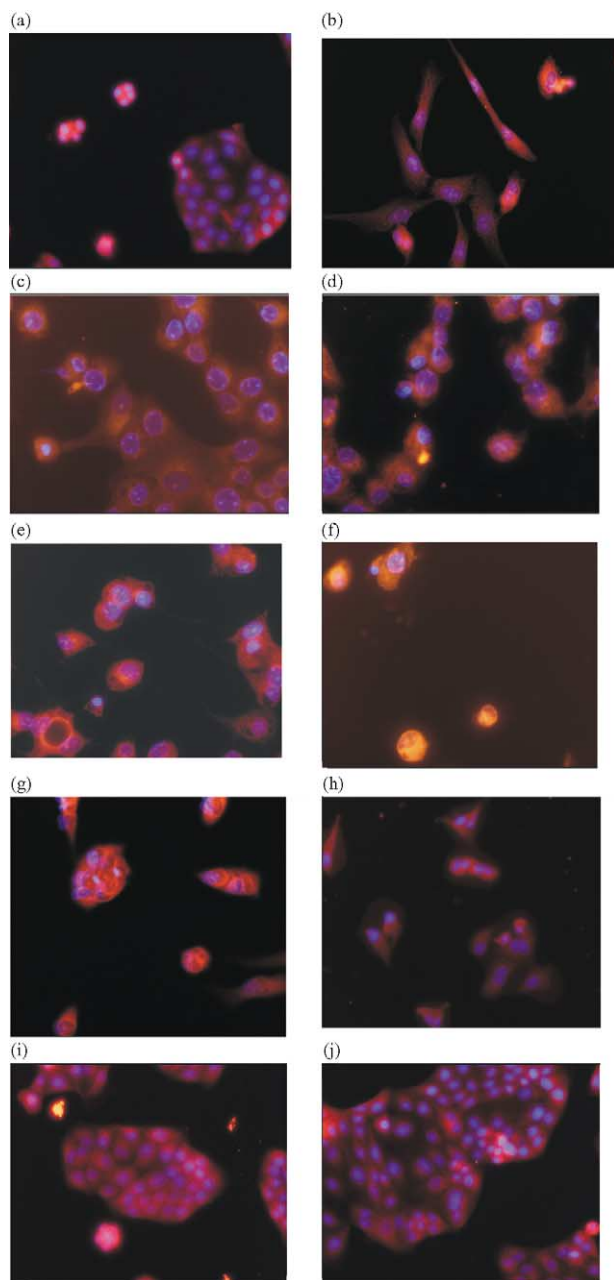
Figure 5. Effects of different inhibitors on cell lines: (a) negative control, MDCK (wild-type cell, without inhibitor); (b) negative control, MDCK-f3 (tumour cell, without inhibitor); (c) **7** (100 μM), MDCK-f3; (d) **8** (100 μM), MDCK-f3; (e) **9** (100 μM), MDCK-f3; (f) **6** (100 μM), MDCK-f3; (g) **53** (100 μM), MDCK-f3; (h) **6** (50 μM), MDCK-f3; (i) **6** (100 μM), MDCK; (j) **53** (100 μM), MDCK.

Several compounds induced apoptosis in a Ras-transformed tumour cell line with no effect on the corresponding untransformed cells. Only in one case, however, correlated this biological activity directly with farnesyltransferase inhibition.

Based on these findings new opportunities in the chemical biology of Ras proteins could be opened up, in particular for the determination of the crucial but yet unidentified target of farnesyltransferase inhibitors.

Experimental

The used chemicals, buffers and dyes were purchased from Sigma or Fluka. The [³H]-FPP-solution was supplied by New England Nuclear. The precipated K-ras was filtered with filtermates (type B) in a Tomtec™-Harvester and the transferred radioactivity was measured by a Wallac™ 1024 Betaplate szintillator. The fluorescence development was recorded on a Fluoroscan-FL Fluorometer of Ascent Labsystems (filter: $\lambda_{ex} = 355$ nm, $\lambda_{em} = 460$ nm). For the fluorescence microscopy an Axiophot fluorescence microscope (Zeiss) was used.

Molecular modelling

The coordinates of the rat farnesyltransferase structure were taken from the PDB (1JCR). For the purpose of comparison, the structure without a ligand (1FT1) was used. Addition of hydrogens was carried out using the algorithms implemented in WitnotP[22] and minimized using CHARMM[23] (200 cycles, steepest descent) keeping backbone atoms fixed. For this and all subsequent minimizations, the atoms of residues coordinating the essential Zn^{2+} were fixed in their respective positions. The structures of the inhibitors were created using the graphic tools within WitnotP and minimized using CHARMM. Manual Docking into the active site of farnesyltransferase. During minimization (conjugate gradient, 10,000 cycles, Gradient 0.05), all atoms located more than 8 Å from any inhibitor atom were fixed in their positions. All other atoms were free to move. The surfaces in the figures are displayed as 'solvent accessible surfaces', the probe radius was set to 1.4 Å. Measurement of the lenths and angles of the H-bonds mentioned above was carried out with tools in WitnotP. The surface color was determined as follows: The SA surface of residues located within 4 Å of atoms of the FPP moiety in the 1JCR structure were colored green. The SA surface of residues located within 4 Å of atoms of the CVFM peptide were colored yellow. The hydrophobicity maps were created using HYDROMAP.[24]

Radioactivity-based PFT inhibition assay

To a solution of 100 μL of K-ras (0.27 mg l⁻¹), human PFT in the buffer medium (8.6 mM MgCl₂, 17.1 μM ZnCl₂, 1.32 mg mL⁻¹ DTT, 86 mM Tris/HCl pH = 8.0) were pipetted 10 μL of a [³H]-FPP-solution (3.3 mM, 15–30 Ci mmol⁻¹) and the solution was incubated for 30 min at 37 °C. Then the reaction was stopped by addition of 100 μL of a solution of concentrated HCl in ethanol (15%), the precipitated ras-protein was filtered and the radioactivity was measured.

Fluorescence-based PFT inhibition assay

Per well (96 well-plate) 20 μL of a solution of rat-PFT (2.6 μM in the buffer medium indicated below) was added by the dispenser function of the apparatus to 180 μL of a preincubated solution (at 30 °C) of FPP (10 μM), Dansyl-GCVLS-peptide (10 μM), varied concentrations of the inhibitor in 20 μL of methanol and 160

µL of buffer solution (50 mM Tris/HCl pH 7.5, 5 mM DTE, 10 µM ZnCl$_2$, 5 mM MgCl$_2$, 0.2% (w,v) *n*-octyl-β-D-glucopyranoside) and then the fluorescence development was recorded for 5 min at 30 °C.

Activity assay against MDCK-f3-tumor cells

To MDCK-f3 cells in 500 µL of medium with a density of 5×10^3 cells/mL on an object carrier were added varied concentrations (20, 50 and 100 µM, in 0.5 µL DMSO) of the appropriate substances. After incubation for 6 h at 37 °C the cells were washed with PBS-buffer, fixed and permeabilized by treatment with cold methanol/acetone (1:1) for 30 min. Afterwards, the cells were washed again with PBS (3×10 min), then incubated with PBS/BSA 2% for 30 min, followed by staining with the fluorescence dye TRITC coupled with an actin specific antibody for 1 h. After washing with PBS (3×10 min) the nucleus was stained with DAPI (1:20.000), followed by washing with PBS (3×10 min) and addition of moviol. The effects were then investigated by fluorescence microscopy.

Activity assay against wild-type MDCK cells

The test was performed as described above for the MDCK-f3-cells. Herein a MDCK cell density of 1×10^4 cells/mL was used.

Acknowledgements

References and Notes

1. (a) Waldmann, H.; Thutewohl, M. *Top. Curr. Chem.* **2001**, *211*, 117. (b) Wittinghofer, A.; Waldmann, H. *Angew. Chem., Int. Ed. Engl.* **2000**, *39*, 4192. Wittinghofer, A.; Waldmann, H. *Angew. Chem.* **2000**, *112*, 4360.
2. Sebti, S. M.; Hamilton, A. D. *Oncogene* **2000**, *19*, 6584.
3. (a) Cox, A. D.; Der, C. J. *Biochim. Biophys. Acta* **1997**, *1333*, F51. (b) Zhang, F. L.; Casey, P. J. *Annu. Rev. Biochem.* **1996**, *65*, 241.
4. Levitzki, A. *Eur. J. Biochem.* **1994**, *226*, 1.
5. (a) Schlitzer, M.; Böhm, M.; Sattler, I.; Dahse, H.-M. *Bioorg. Med. Chem.* **2000**, *8*, 1991. (b) Manne, V.; Yan, N.; Carboni, J. M.; Tuomari, A. V.; Ricca, C. S.; Gullo Brown, J.; Andahazy, M. L.; Schmidt, R. J.; Patel, D.; Zahler, R.; Weinmann, R.; Der, C. J.; Cox, A. D.; Hunt, J. T.; Gordon, E. M.; Barbacid, M.; Seizinger, B. R. *Oncogene* **1995**, *10*, 1763.
6. Sorbera, L. A.; Fernandez, R.; Castaner, J. *Drugs Future* **2001**, *26*, 453.
7. Leonard, D. M. *J. Med. Chem.* **1997**, *40*, 2971.
8. Shiomi, K.; Yang, H.; Inokoshi, J.; Van der Pyl, D.; Nakagawa, A.; Takeshima, H.; Omura, S. *J. Antibiot.* **1993**, *46*, 229.
9. (a) Hinterding, K.; Hagenbuch, P.; Rétey, J.; Waldmann, H. *Angew. Chem., Int. Ed.* **1998**, *37*, 1236. Hinterding, K.; Hagenbuch, P.; Rétey, J.; Waldmann, H. *Angew. Chem.* **1998**, *110*, 1298. (b) Hinterding, K.; Hagenbuch, P.; Rétey, J.; Waldmann, H. *Chem. Eur. J.* **1999**, *5*, 227.
10. (a) Part of this work was published in a preliminary form: Thutewohl, M.; Kissau, L.; Popkirova, B.; Karaguni, I.-M.; Nowak, T.; Bate, M.; Kuhlmann, J.; Müller, O.; Waldmann, H. *Angew. Chem. Int. Ed.* **2002**, *41*, 3616. (b) Thutewohl, M.; Waldmann, H. Accompanying article in this issue. doi:10.1016/S0968-0896(03)00159-7
11. Pompliano, D. L.; Rands, E.; Schaber, M. D.; Mosser, S. D.; Anthony, N. J.; Gibbs, J. B. *Biochemistry* **1992**, *31*, 3800.
12. Pompliano, D. L.; Gomez, R. P.; Anthony, N. J. *J. Am. Chem. Soc.* **1992**, *114*, 7945.
13. The screening was performed on a plate reader with an optical filter system which required a change in excitation and emission wavelength. The used wavelength ($\lambda_{ex} = 355$ nm, $\lambda_{em} = 460$ nm) resulted only in a slight loss of intensity.
14. Bell, I. M. *Exp. Opin. Ther. Pat.* **2000**, *10*, 1813.
15. Long, S. B.; Casey, P. J.; Beese, L. *Structure* **2000**, *8*, 209.
16. Majeux, N.; Scarsi, M.; Tenette-Souaille, C.; Caflisch, A. *Perspect. Drug Discov. Des.* **2000**, *20*, 145.
17. Dudev, T.; Lim, C. *J. Am. Chem. Soc.* **2000**, *122*, 11146.
18. Dolence, J. M.; Cassidy, P. B.; Mathis, J. R.; Poulter, C. D. *Biochemistry* **1995**, *34*, 16687.
19. Karaguni, I.-M.; Glüsenkamp, K.-H.; Langerak, A.; Geisen, C.; Ullrich, V.; Winde, G.; Möröy, T.; Müller, O. *Bioorg. Med. Chem. Lett.* **2002**, *12*, 709.
20. Behrens, J.; Mareel, M.; Van Roy, F. M.; Birchmeier, W. *J. Cell. Biol.* **1989**, *108*, 2435.
21. At 100 µM and higher inhibitor concentrations up to 1 mM no visible effect was observed for MDCK-cells.
22. Widmer, A., WitnotP is a molecular modelling program developed at Novartis AG, comparable with InsightII from Accelrys Inc.
23. Brooks, B. R.; Bruccoleri, R. E.; Olafson, B. D.; States, D. J.; Swaminathan, S.; Karplus, M. *J. Comp. Chem.* **1983**, *4*, 187.
24. Scarsi, M.; Majeux, N.; Caflisch, A. *Proteins. Struct. Funct. Genet.* **1999**, *37*, 565.